Available online at www.sciencedirect.com
ScienceDirect
Ceramics International 37 (2011) 3211–3216
CERAMICS INTERNATIONAL
www.elsevier.com/locate/ceramint

Study on the preferred orientations of nearly cubic PZT particles synthesized by hydrothermal methods using $TiCl_3$ reagent

Seok Han Kim, Sridhar Komarneni *

Materials Research Institute, The Pennsylvania State University, University Park, PA 16802, USA

Received 7 December 2010; received in revised form 14 March 2011; accepted 14 March 2011
Available online 27 May 2011

Abstract

Various parameters such as gel composition, aging, organic additive, and heating method affected the preferred orientation of nearly cubic PZT particles that were prepared by hydrothermal methods using $TiCl_3$ as a Ti^{3+} source, at relatively low temperatures of 100–140 °C. The newly found synthetic conditions could be used to develop specially orientated PZT particles, which may be useful in growing oriented films, for example, by electrophoretic deposition.

Keywords: D. PZT; Hydrothermal synthesis; Preferred orientation; $TiCl_3$

1. Introduction

Lead zirconate titanate ($Pb(Zr_xTi_{1-x})O_3$; PZT) was extensively studied because of its excellent ferroelectric, piezoelectric, pyroelectric, and dielectric properties for applications in pyroelectric infrared detectors, piezoelectric actuators, and micro-electro-mechanical systems (MEMS) [1,2]. PZT particles and films were generally synthesized by several techniques such as mixed oxide, sputtering, chemical vapor deposition, sol–gel, and others [3–5]. The electrical properties such as pyroelectric coefficient and dielectric constants of the PZTs were affected by the preferred orientation of the films and their preferred orientation [3–7]. The preferred orientations of PZT obtained by the techniques could be controlled by choosing appropriate substrate, deposition method, drying temperature, and other synthetic parameters [6,7].

Hydrothermal methods for PZT synthesis were investigated to get very thick PZT films with high deposition rates and relatively low-temperatures (<250 °C) were used to make PZT films with low number of defects [8–18]. In addition, the preparation of PZT by hydrothermal methods was expected to save energy compared with that of conventional mixed oxide method, which uses much higher processing temperatures.

Hydrothermal method consists of two steps, ''nucleation'' and ''crystal growth''. Although this method was used to prepare PZT thin films on TiO_2 substrates with ferroelectric properties, it was difficult to control the chemical composition and the phase of the PZT films [15]. The thicknesses of the PZT films synthesized by the two-step hydrothermal methods were controlled by repeated hydrothermal treatments [16]. The hydrothermal method for PZT thin films was later simplified by omitting ''nucleation'' process and the Zr/(Zr + Ti) ratio of the film could be controlled by changing the ionic composition of the solution [17]. Recently, (1 0 0)-oriented PZT films on single-crystal $SrTiO_3$ (1 0 0) substrates were deposited by hydrothermal methods at 150 °C for 24 h and highly (1 0 0)-oriented PZT nanostructures were hydrothermally synthesized on $SrTiO_3$ (1 0 0) substrates at 160 °C [18,19]. Various conditions such as concentration and stirring speed during the hydrothermal methods affected the sizes, phase purity, and crystal quality of the PZT films and particles [18]. Additionally, phase-pure PZT precipitations were synthesized by controlling synthetic parameters including Zr and Ti source, Pb source, temperature, KOH concentration, and pH during the hydrothermal process [20]. These results imply that the reaction conditions affect the phase, purity, and size of PZT films and particles. However, the effect of synthetic conditions on the preferred orientations of PZT films and particles was rarely studied using the hydrothermal methods when compared to the studies related to the effect of substrate.

* Corresponding author.
E-mail address: komarneni@psu.edu (S. Komarneni).

0272-8842/$36.00
doi:10.1016/j.ceramint.2011.05.091

However, well-optimized hydrothermal synthesis conditions can be a primary strategy to control the physicochemical properties such as size and preferred orientation of PZT particles and films. Here, we report the synthetic conditions for growing hydrothermal PZT particles of preferred orientation but these conditions could also be applied to hydrothermally synthesized PZT films because of similar crystal growth mechanism.

Very recently a Ti^{3+} reagent, $TiCl_3$, was used by us [14] to make PZT particles instead of Ti^{4+} reagents such as $TiCl_4$, TiO_2, and $(C_4H_9O)_4Ti$. These results postulated that the synthetic intermediate prepared by Ti^{3+} reagent had more defects and therefore, easily reacted with Zr reagent at a lower temperature of 110 °C than those by Ti^{4+} reagents [14].

In this work, various conditions such as mineralizers, water contents, aging times and temperatures, and heating methods were studied for hydrothermal PZT synthesis using a Ti^{3+} reagent in order to understand and control the physical and chemical properties including preferred orientations of PZT particles. The oriented PZT particles synthesized here may be useful for making oriented films of PZT by electrophoretic deposition [21].

2. Experimental

2.1. Materials

The reagents were $TiCl_3$ (20% $TiCl_3$ in 3% HCl solution, Alfa Aesar), $Pb(NO_3)_2$ (99.0%, Alfa Aesar), $ZrOCl_2{\cdot}8H_2O$ (98%, Alfa Aesar), KOH (85%, Alfa Aesar), NaOH (97.0%, Alfa Aesar), RbOH (87.5%, Alfa Aesar), CsOH (87.5%, Alfa Aesar), oleic acid (Alfa Aesar), stearic acid (95%, Aldrich), sodium stearate (Alfa Aesar), and deionized water.

2.2. Synthesis of PZT particles

The typical gel compositions for PZT syntheses prepared here were $0.63Pb(NO_3)_2 0.32ZrOCl_2 0.29TiCl_3 10MOHxH_2O$, where M is K, Na, Rb, or Cs and x is 67, 100, or 125 (Table 1). Each synthetic gel was prepared by the following procedure. $TiCl_3$ solution was firstly mixed with deionized water. The other reagents were then added to the Ti containing solution in the order of $ZrOCl_2{\cdot}8H_2O$, $Pb(NO_3)_2$, MOH, and others such as oleic acid or stearic acid and sodium stearate while stirring. Four samples, runs 8, 9, 14, and 15, were additionally aged for 24 h (Table 1). Each of the mixtures was charged into a Teflon-lined 125-mL autoclave and then heated in a conventional oven or using a microwave digestion system (model no. MARS-5, CEM-Corporation) in the temperature range of 100–140 °C for 1–24 h without stirring under autogenous pressure (Table 1). After the vessels were cooled to room temperature, the white powders obtained by hydrothermal reactions were collected and washed repeatedly with deionized water by centrifugation at 2000 rpm for ~10 min. The solids were dried at 60 °C before characterization.

2.3. Characterization

Powder X-ray diffraction (XRD) patterns were obtained on a PANalytical X'Pert MPD diffractometer operated at 45 kV

Table 1
Representative synthesis conditions and results.

Run	Gel composition[a]			Aging		Crystallization		PZT
	M	Organic additives	x	T (°C)	t (h)	T (°C)	t (h)	Preferred orientation[b]
1	K		67	–	–	140	24	(1 1 0) > (1 0 1) > (1 0 0)/(0 0 1)
2[c]	K		67	–	–	140	24	(1 0 1) = (1 1 0) > (0 0 1) > (1 0 0)
3	Na		67	–	–	140	24	(1 0 1) > (1 1 0) = (1 0 0)/(0 0 1)
4	Rb		67	–	–	140	24	–
5	Cs		67	–	–	140	24	–
6	K		100	–	–	140	24	(1 0 1) > (1 1 0) = (1 0 0)/(0 0 1)
7	K		125	–	–	140	24	(1 0 1) > (1 1 0) = (1 0 0)/(0 0 1)
8	K		67	30	24	140	24	(1 1 0) > (1 0 1) > (1 0 0)/(0 0 1)
9	K		67	50	24	140	24	(1 1 0) > (1 0 1) > (1 0 0)/(0 0 1)
10[d]	K	Oleic acid	67	–	–	140	24	(1 1 0) > (1 0 1) > (1 0 0)/(0 0 1)
11[d]	K	Stearic acid, sodium stearate	67	–	–	140	24	(1 1 0) > (1 0 1) > (1 0 0)/(0 0 1)
12[d]	Na	Oleic acid	67	–	–	140	24	(1 0 1) > (1 1 0) = (1 0 0)/(0 0 1)
13[d]	Na	Stearic acid, sodium stearate	67	–	–	140	24	(1 0 1) > (1 1 0) = (1 0 0)/(0 0 1)
14[d]	K	Oleic acid	67	30	24	140	24	(1 1 0) > (1 0 1) = (1 0 0)/(0 0 1)
15[d]	K	Stearic acid, sodium stearate	67	30	24	140	24	(1 1 0) = (1 0 0)/(0 0 1) > (1 0 1)
16[e]	K		67	–	–	100	1	–
17[e]	K		67	–	–	100	3	–
18[e]	K		67	–	–	100	5	(1 1 0) > (1 0 0)/(0 0 1) > (1 0 1)
19[e]	K		67	–	–	100	10	(1 1 0) > (1 0 0)/(0 0 1) > (1 0 1)

[a] Gel compositions for runs prepared here are $0.63Pb(NO_3)_2 0.32ZrOCl_2 0.29TiCl_3 10MOHxH_2O$ where M is K, Na, Rb, or Cs and x is 67, 100, or 125.
[b] The orders of preferred orientations for each PZT product considering with the peak intensities of XRD patterns.
[c] Prepared by a different mixing procedure. $TiCl_3$ reagent was finally added to the synthetic gel prepared by mixing all the other reagents.
[d] The synthetic gels for runs 10–15 contain organic additives such as oleic acid (OA), stearic acid (SA), and sodium stearate (SS). The gel composition for runs 10, 12, and 14 is $0.63Pb(NO_3)_2 0.32ZrOCl_2 0.29TiCl_3 10KOH 0.34OA 67H_2O$. The gel composition for runs 11, 13, and 15 is $0.63Pb(NO_3)_2 0.32ZrOCl_2 0.29TiCl_3 10KOH 0.08SA 0.06SS 67H_2O$.
[e] Prepared by microwave-hydrothermal process.

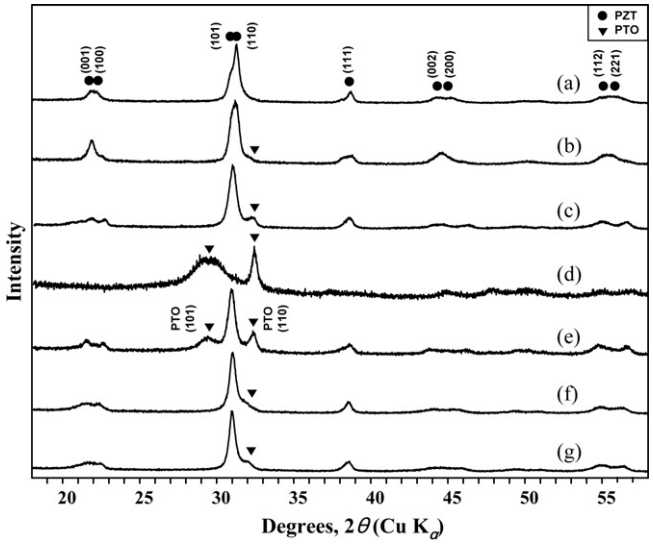

Fig. 1. Powder XRD patterns for products: (a–g) are from runs 1 to 7, respectively (see Table 1).

voltage and 40 mA current with a PIXcel detector and Cu Kα radiation. Scanning electron microscope (SEM) and transmission electron microscope (TEM) images were observed by Hitachi S-3500N and Philips 420 microscopes, respectively. TEM specimens were prepared by depositing a drop of the ethanol solution of PZT sample on a 300 mesh copper grid coated with an amorphous carbon film and evaporating the solvent in air at room temperature.

3. Results and discussion

3.1. Mineralizer effect

The synthetic conditions and results for runs 1–5 using various inorganic alkali hydroxide reagents, KOH, NaOH, RbOH, or CsOH, are described in Table 1 and the XRD patterns are shown in Fig. 1. The XRD peaks (degrees, 2θ) near 21.7°, 22.3°, 30.9°, 31.3°, and 38.7° were generated by X-ray diffraction of (0 0 1), (1 0 0), (1 0 1), (1 1 0), and (1 1 1) planes of PZT, respectively [8,9,11,12]. The reflections at *ca.* 29.3°, 32.4°, and 37.1° (Fig. 1e) indicated (1 0 1), (1 1 0), and (0 0 2) planes of PTO (lead titanium oxide; $PbTi_{0.8}O_{2.6}$), respectively [11]. The XRD patterns showed that PZT particles were obtained in runs 1–5 containing KOH, KOH, NaOH, RbOH, and CsOH, respectively (Fig. 1). The run 2 sample was prepared by a different mixing procedure as follows: $TiCl_3$ solution was added to the synthetic gel in the final step instead of in the first step as per run 1. However, the XRD pattern for run 4 using RbOH showed only two reflections at 29.4° and 32.4° related to PTO (Fig. 1d). Detectable amounts of PTO particles were also found as impurities in run 5 using CsOH (Fig. 1e). Runs 1–3 had small reflections or shoulders at 32.4° in their XRD patterns (Fig. 1a–c). However, the other reflections related to PTO were not found in these patterns. This means that the amounts of PTO impurities for runs 1–3 were quite small even though different mixing procedures were used.

Table 1 gives the orders of preferred orientations for each run. The preferred orientations of the PZT particles obtained from runs 1–3 were estimated by considering relative XRD peak intensities for these runs (Fig. 1a–c) near 21.7°, 22.3°, 30.9°, and 31.3° related to (0 0 1), (1 0 0), (1 0 1), and (1 1 0) planes of PZT, respectively. The highest XRD reflection of run 1 using KOH was at 31.3° (Fig. 1a) and this indicated that the main orientation was (1 1 0). In contrast, the PZT (1 0 1) peaks for runs 3 (Fig. 1c) and 5 (Fig. 1e), were higher than their (1 1 0) peaks. This result implied that the inorganic alkali hydroxide reagents of KOH, NaOH, CsOH, and RbOH affected the preferred orientations of PZT particles during synthesis. However, run 2 obtained from a different mixing procedure had the same intensity of XRD peaks for both (1 0 1) and (1 1 0) planes (Fig. 1b).

The morphologies and sizes of the typical PZT particles obtained from runs 1 and 10 were examined by SEM (Fig. 2a) and TEM (Fig. 2b), respectively. The PZT particles obtained here showed aggregated cubic- or rectangular parallelepied-shape and average sizes of 80 nm to 1 μm on an edge. The average sizes of the PZT particles of run 1 using KOH and run 3 using NaOH were 0.8 μm and 80 nm on an edge, respectively, and that of a sample using a mixture of NaOH and KOH was 0.5 μm that was quite similar to the mean of the PZT sizes for runs 1 and 3 as reported previously by us [14]. The average

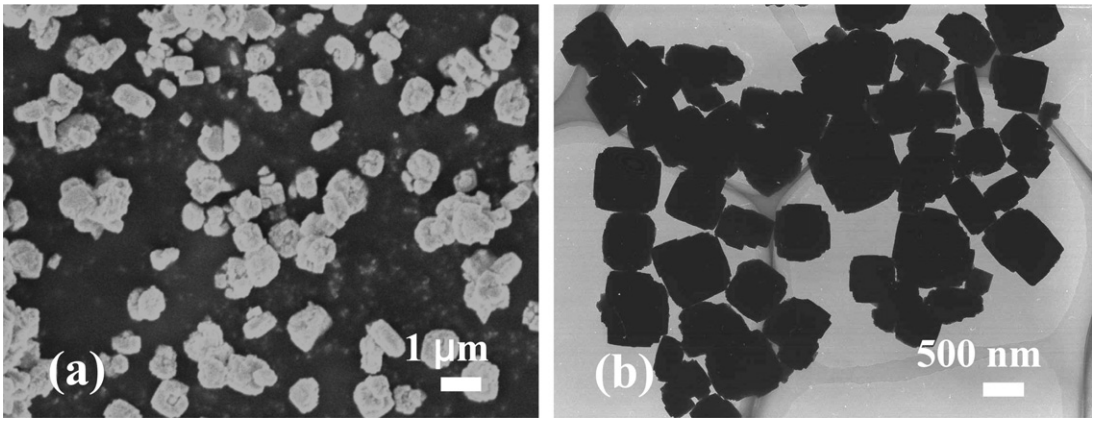

Fig. 2. Typical SEM (a) and TEM (b) images for PZT particles obtained here (see Table 1 runs 1 and 10, respectively).

sizes of PZT particles synthesized by this hydrothermal method were affected by mineralizers such as KOH and NaOH as a result of the different solubility of gels in each mineralizer and thus affecting the number of nuclei produced during nucleation step [14].

3.2. Water content effect

Runs 6 and 7 were prepared for finding the role of water content on PZT crystallization (Table 1). In contrast with run 1, the standard water content of this work with $x = 67$, runs 6 and 7 had more water (Table 1) in their gels ($x = 100$ and 125, respectively). XRD patterns for runs 6 and 7 with higher water contents indicated that PZT was obtained with high yields (Fig. 1f and g). Small XRD peaks were also found near 32.1° and these were probably related to (1 1 0) plane of PTO for runs 6 and 7 (Fig. 1f and g, see arrows). However, other XRD peaks related to PTO were not found. This implied that quite a small amount of PTO or its precursor particles were in the batches of runs 6 and 7 as impurities. Run 1 consisted of almost pure PZT particles although an evidence of PTO impurities was also found in its XRD pattern as a very small shoulder near 32.1° (Fig. 1a). The order of higher intensities of the peak near 32.1° was: run 7 > run 6 > run 1 (Fig. 1). This meant that the amounts of PTO or its precursor particles were found to increase in proportion to the water content in the synthetic gels.

XRD intensities for (1 0 1) near 30.9° were higher than that for (1 1 0) near 31.3° for both runs 6 and 7, which was different from run 1 that had its highest peak intensity for (1 1 0) (Fig. 1). The highest XRD peaks for runs 6 and 7 indicated that (1 0 1) orientated PZT could be obtained from synthetic conditions with higher water contents (Fig. 1f and g).

3.3. Aging and organic additive effect

Three samples, runs 8–10, were prepared with different aging conditions to find the aging effect on PZT crystallization (Table 1). Runs 8 and 9 were prepared by aging at 30 and 50 °C, respectively, for 24 h. No difference of the XRD patterns among runs 1, 8, and 9 was found, which suggested that aging at these temperatures had no effect on PZT particles (Figs. 1a, 3a, and b). An organic additive, oleic acid, was used for preparing runs 10, 12, and 14 (Table 1). Both runs 10 and 14 obtained from KOH-containing gels with and without aging, respectively, gave no significant difference in their XRD patterns (Fig. 3c and g) in comparison with the XRD pattern of run 1 without aging (Fig. 1a). However, run 12 obtained using oleic acid and NaOH mineralizer without aging led to a change in the preferred orientation (Fig. 3e). XRD pattern for run 12 had the highest peak intensity at (1 0 1) position due to the effect of NaOH mineralizer. This behavior was also found in the XRD pattern for run 13 synthesized using stearic acid, sodium stearate, and NaOH mineralizer (Fig. 3f). NaOH mineralizer apparently led to the primary effect on the preferred orientation of PZT particles for PZT synthesis.

Runs 11, 13, and 15 were prepared using other organic additives, stearic acid and sodium stearate, with or without aging (Fig. 3d, f, and h). A test run (run 11) obtained by a similar recipe of run 1 with additional organic reagents, stearic acid and sodium stearate, and without aging did not change the preferred orientation (Fig. 3d) compared with the XRD pattern of run 1 obtained with no special reagent (Fig. 1a). Run 13 prepared using stearic acid, sodium stearate, and NaOH mineralizer without aging had the highest peak intensity at (1 0 1) position on its XRD pattern probably due to the effect of Na mineralizer on the preferred PZT orientation (Fig. 3f). Run 15 obtained by a special condition, a combination of aging at 30 °C for 24 h and organic additives, stearic acid and sodium stearate, made a distinct change in the preferred orientation of PZT (Table 1 and Fig. 3h). Run 15 had the highest intensity of XRD peak at 21.9° among all runs studied here and the peak position was similar to the mean of (0 0 1)/(1 0 0) peaks of PZT (Fig. 3h). The combined condition of aging and organic additives was the key in promoting (0 0 1)/(1 0 0)-orientated PZT growth.

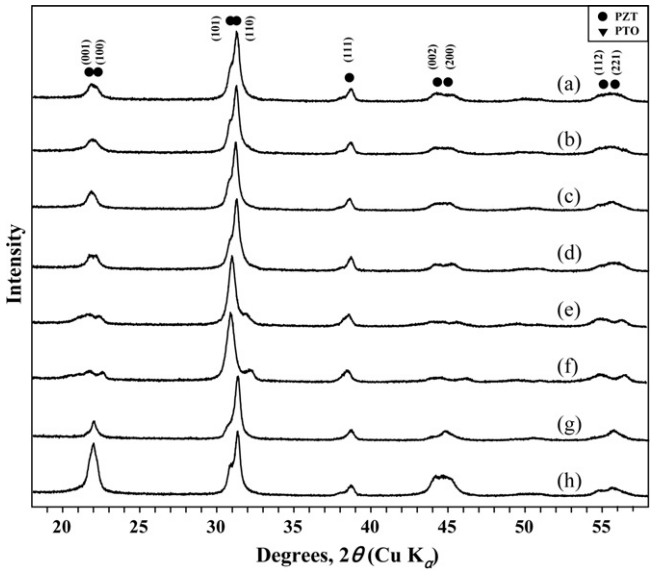

Fig. 3. Powder XRD patterns for products: (a–h) are from runs 8 to 15, respectively (see Table 1).

3.4. Microwave hydrothermal synthesis

Fig. 4 shows the XRD patterns for PZT batches, runs 16–19, synthesized from microwave hydrothermal method during its crystallization (Table 1). Similar to the changes of the XRD patterns for PZT particles obtained by conventional hydrothermal method [14], no PZT peak was found at the initial stages of the microwave hydrothermal crystallization. However, PTO (1 0 1) and (1 1 0) peaks were found near 29.3° and 32.5°, respectively, at the initial step (1 h) (Fig. 4a). The PTO peaks decreased during crystallization and only trace peaks remained at the longest crystallization time (Fig. 4d). In contrast with PTO peaks, the PZT (0 0 1)/(1 0 0) and (1 0 1)/(1 1 0) peaks near 22° and 31° increased in their intensities with increased time of crystallization. This behavior was also found with the PZT particles obtained by conventional hydrothermal

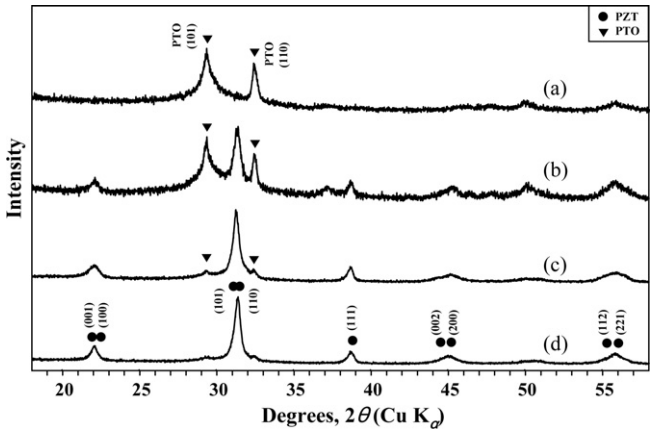

Fig. 4. Powder XRD patterns for products: (a–d) are from runs 16 to 19 that are crystallized at 100 °C for 1, 3, 5, and 10 h, respectively, using microwave-hydrothermal process (see Table 1).

method [14], and the crystallization rates for both conventional and microwave runs were not significantly different [14]. However, the PZT peaks near 31° were at 30.7° and 31.3° for conventionally heated runs but at 31.3° for microwave heated runs [14]. The PZT synthesized by microwave hydrothermal technique had mainly (1 1 0) orientation with little or no (1 0 1) orientation.

3.5. Crystallization temperature effect

Two sets of PZT using KOH and mixed NaOH/KOH mineralizers were prepared at 100–160 °C in our previous study [14]. XRD peaks near 31° related to (1 0 1) and (1 1 0) planes of PZT shifted with increasing crystallization temperature prepared from KOH-containing gels although the XRD patterns resulting from mixed KOH/NaOH gels did not change with temperature (Figs. 3 and 4 of Ref. [14]). Each of the other runs prepared at 110, 120, 140, and 160 °C, respectively, had two peaks at 30.8° and 31.3° that were from (1 0 1) and (1 1 0) of PZT, respectively. The intensity of (1 0 1) peak near 30.8° for these runs decreased and that of (1 1 0) peak near 31.3° increased when the crystallization temperature increased. Thus crystallization temperature led to some effects on (1 1 0) and (1 0 1) orientations during PZT crystal growth for KOH containing runs only. However, the XRD patterns for mixed NaOH/KOH containing runs treated at 100–160 °C were quite similar with no differences in preferred orientation of the PZT particles. These results indicated that preferred orientation occurred with increasing crystallization temperature when PZT particles were obtained from KOH containing synthetic gels.

3.6. Summary for the preferred orientations of PZT particles

XRD patterns for representative runs 1, 3, 6, 15, and 19 showed different preferred orientations for PZT particles in Figs. 1a, c, f, 3h, and 4d, respectively. There were several interesting synthetic conditions which promoted orientations of (0 0 1)/(1 0 0), (1 0 1), or (1 1 0) for PZT. Run 1 had both (1 0 1) and (1 1 0) PZT peaks at 30.7° and 31.3°, respectively (Fig. 1a). However, XRD patterns for runs 3 (Fig. 1c) prepared by using NaOH and 6 (Fig. 1f) prepared by using KOH with higher water content (100 H_2O), respectively, had preferred (1 0 1) PZT peaks between 30.8° and 31.0° with little or no (1 1 0) peak near 31.3° (Fig. 1c and f). In contrast, run 19 obtained by microwave hydrothermal synthesis for 10 h did not show (1 0 1) PZT peak but showed a preferentially orientated (1 1 0) peak at 31.3° (Fig. 4d). Run 15 prepared by using a combined condition of aging at 30 °C and using stearic acid and sodium stearate, had the highest (0 0 1)/(1 0 0) PZT peak among all the runs studied here (Fig. 3h). The synthetic parameters studied here may provide useful information to design a unique hydrothermal method for making PZT particles of special orientation.

References

[1] R. Ramesh, Thin Film Ferroelectric Materials and Devices, Kluwer, Boston, 1997.
[2] S.S. Roy, H. Gleeson, C.P. Shaw, R.W. Whatmore, Z. Huang, Q. Zhang, S. Dunn, Growth and characterization of lead zirconate titanate (30/70) on indium tin oxide coated glass for oxide ferroelectric-liquid crystal display application, Integr. Ferroelectr. 29 (2000) 189–213.
[3] K. Sreenivas, M. Sayer, Characterization of lead zirconate titanate thin films deposited from multi-element metal targets, J. Appl. Phys. 64 (1988) 1484–1493.
[4] J.-W. Moon, S. Tazawa, K. Shinozaki, N. Wakiya, N. Mizutani, Impact of thin $SrTiO_3$ seed layer to achieve low-temperature crystallization below 300 °C and ferroelectricity of lead zirconate titanate thin film, Appl. Phys. Lett. 89 (2006) 202907.
[5] G. Yi, Z. Wu, M. Sayer, Preparation of lead zirconate titanate thin films by sol gel processing: electrical, optical, and electro-optic properties, J. Appl. Phys. 64 (1988) 2717–2724.
[6] K. Aoki, Y. Fukuda, K. Numata, A. Nishimura, Dielectric properties of (1 1 1) and (1 0 0) lead-zirconate-titanate films prepared by sol–gel technique, Jpn. J. Appl. Phys. 33 (1994) 5155–5158.
[7] C.J. Kim, D.S. Yoon, J.S. Lee, C.G. Choi, W.J. Lee, K. No, Electrical characteristics of (1 0 0), (1 1 1), and randomly aligned lead zirconate titanate thin films, J. Appl. Phys. 76 (1994) 7478–7482.
[8] Y. Lin, Y. Liu, H.A. Sodano, Hydrothermal synthesis of vertically aligned lead zirconate titanate nanowire arrays, Appl. Phys. Lett. 95 (2009) 122901.
[9] G. Xu, W. Jiang, M. Qian, X. Chen, Z. Li, G. Han, Hydrothermal synthesis of lead zirconate titanate nearly free-standing nanoparticles in the size regime of about 4 nm, Cryst. Growth Des. 9 (2009) 13–16.
[10] D.J. You, W.W. Jung, S.K. Choi, Domain structure in a micron-sized $PbZr_{1-x}Ti_xO_3$ single crystal on a Ti substrate fabricated by hydrothermal synthesis, Appl. Phys. Lett. 84 (2004) 3346–3348.
[11] Z.-C. Qiu, J.-P. Zhou, G. Zhu, P. Liu, X.-B. Bian, Hydrothermal synthesis of $Pb(Zr_{0.52}Ti_{0.48})O_3$ powders at low temperature and low alkaline concentration, Bull. Mater. Sci. 32 (2009) 193–197.
[12] S. Harada, S. Dunn, Low temperature hydrothermal routes to various PZT stochiometries, J. Electroceram. 20 (2008) 65–71.
[13] S. Komarneni, Q. Li, K.M. Stefansson, R. Roy, Microwave-hydrothermal processing for synthesis of electroceramic powders, J. Mater. Res. 8 (1993) 3176–3183.
[14] S.H. Kim, S. Komarneni, Synthesis of PZT fine particles using Ti^{3+} precursor at a low hydrothermal temperature of 110 °C, Ceram. Int., 37 (2011) 1101–1107.
[15] K. Shimomura, T. Tsurumi, Y. Ohba, M. Daimon, Preparation of lead zirconate titanate thin film by hydrothermal method, Jpn. J. Appl. Phys. 30 (1991) 2174–2177.
[16] Y. Ohba, M. Miyauchi, T. Tsurumi, M. Daimon, Analysis of bending displacement of lead zirconate titanate thin film synthesized by hydrothermal method, Jpn. J. Appl. Phys. 32 (1993) 4095–4098.

[17] T. Morita, T. Kanda, Y. Yamagata, M. Kurosawa, T. Higuchi, Single process to deposit lead zirconate titanate (PZT) thin film by a hydrothermal method, Jpn. J. Appl. Phys. 36 (1997) 2998–2999.
[18] W.L. Suchanek, M. Lencka, L. McCandlish, R.L. Pfeffer, M. Oledzka, K. Mikulka-Bolen, G.A. Rossetti Jr., R.E. Riman, Hydrothermal deposition of ⟨0 0 1⟩ oriented epitaxial $Pb(Zr,Ti)O_3$ films under varying hydrodynamic conditions, Cryst. Growth Des. 5 (2005) 1715–1727.
[19] S. Dunn, S. Harada, Hydrothermal deposition of heteroepitaxial lead zirconate titanate nanostructures and thin films, J. Eur. Ceram. Soc. 28 (2008) 2747–2753.
[20] M.M. Lencka, A. Anderko, R.E. Riman, Hydrothermal precipitation of lead zirconate titanate solid solutions: thermodynamic modeling and experimental synthesis, J. Am. Ceram. Soc. 78 (1995) 2609–2618.
[21] J. Van Tassel, C.A. Randall, Electrophoretic deposition and sintering of thin/thick PZT films, J. Eur. Ceram. Soc. 19 (1999) 955–958.